Protist 172 (2021) 125822
http://www.elsevier.de/protis
Published online date

Protist

ORIGINAL PAPER

Evidence for Host Jumping and Diversification of Marine Cephaloidophorid Gregarines (Apicomplexa) Between Two Distantly Related Animals, viz., Crustaceans and Salps

Kevin C. Wakeman [a,1], Shimpei Hiruta [b], Yusuke Kondo [c], and Susumu Ohtsuka [c]

[a]Institute for the Advancement of High Education, Hokkaido University, Japan
[b]Center for Molecular Biodiversity Research, National Museum of Nature and Science, Amakubo 4-1-1, Tsukuba, Ibaraki 305-0005, Japan
[c]Takehara Station, Setouchi Field Science Center, Graduate School of Integrated Sciences for Life, Hiroshima University, 5-8-1 Minato-machi, Takehara, Hiroshima 725-0024, Japan

Submitted November 15, 2020; Accepted June 15, 2021
Monitoring Editor: Frank Seeber

This study examined the evolutionary history and diversity of marine gregarine parasites of pelagic zooplankton, and highlighted a unique example of a host-jumping event of cephaloidophorid gregarines between two distantly related host groups, crustaceans and chordates. *Candacia bipinnata* Giesbrecht, 1889, a free-living calanoid copepod, and a salp, *Salpa fusiformis* Cuvier, 1804, were collected on oceanic research cruises in 2018 and 2019, in the West Pacific aboard TRV SEISUI MARU and TOYOSHIO MARU, respectively. A molecular phylogeny based on 18S rDNA nested the gregarine parasite from *S. fusiformis* among cephaloidophorids, within a clade exclusively comprised of gregarines from crustaceans. The relationship between these groups was underpinned with ultrastructural data including the presence of a septum, and similarities in the apices of the epicytic folds. Subsequently, it was concluded to establish a new combination, *Cephaloidophora* cf. *flava* n. comb (Ex. *Thalicola flava*) and transfer the other two members of the *Thalicola* (also parasites of salps) to the *Cephaloidophora*. This study also attempted to ascertain the origin of cephaloidophorids in *S. fusiformis*. However, the relationship between *Cephaloidophora bipinnatae* n. sp., and *C.* cf. *flava* n. comb. had only modest support.

Key words: Morphology; pelagic organisms; phylogenetics; speciation; ultrastructure.

[1]Corresponding author. fax +81 11 706 4851;
e-mail wakeman.k@oia.hokudai.ac.jp (K.C. Wakeman).

https://doi.org/10.1016/j.protis.2021.125822

Introduction

Most of what we understand about apicomplexans is based on those that directly impact public health and the economy. *Plasmodium*, *Toxoplasma*, and *Babesia*, for example, are well-known apicomplexan parasites of humans and livestock (Seeber and Steinfelder 2016). Marine apicomplexans are ubiquitous parasites in the sea, infesting a wide variety of animals (Desportes and Schrével 2013a, b). It has been estimated that every animal (metazoan) plays host to at least one apicomplexan parasite (Morrison 2009). In fact, some of these parasites are significant when considering the health of marine fisheries and ecosystems (Kristmundsson et al. 2015). Among these, marine gregarines are of special interest because they represent some of the earliest branches in the tree of apicomplexans, and the study of this particular group will aid in our broader understanding of the diversification and radiation of Apicomplexa, as well as the adaption to a parasitic lifestyle from free-living forms (Leander 2008; Moore et al. 2008). Still, the study of gregarine apicomplexans has been largely neglected, in comparison to their human-infecting relatives. Relatively few species (~2000) have been formally described (Adl et al. 2019; Desportes and Schrével 2013a, b) and even fewer among them have been studied with more contemporary methods such as molecular phylogenetics.

The lifecycle of gregarine apicomplexans is one of the characteristics that sets them apart from other 'core' Apicomplexa (coccidians, haemosporidians, piroplasmids). Core Apicomplexa, with very few exceptions, have two hosts during their lifecycle, an intermediate and determinate host; asexual reproduction occurs in the intermediate hosts, while sexual reproduction occurs in the determinate hosts. For instance, in the lifecycle of the malaria-causing apicomplexan *Plasmodium*, humans act as an intermediate host, and mosquitos the determinant (Smith et al. 2002). Gregarines are different because they are homozygous, having only a single host throughout the course of their life history, even in lineages where asexual reproduction (merogony) has been documented. During the sexual lifecycle of gregarines, two or more individuals attach/fuse to each other (syzygy). The syzygy groupings form a gametocyst where the male and female individuals change into their respective gametes. These gametes fuse to form zygotes that eventually form sporozoites (the infection stages). The sporozoite-containing cysts (sporocysts/sporokysts) are released into the environment to be taken up by another, new host (Desportes and Schrével 2013a; Grassé 1953).

What is quite remarkable about marine gregarines (and apicomplexans as a whole), is the large degree to which they are specific to their hosts and host groups. Even prior to the use of molecular data, a high-level of host specificity was observed. A classic study by Ormières (1965) on marine gregarines infecting tunicates, concluded that different tunicate species with overlapping distributions (i.e., living on the same rock) had separate and distinct, yet closely related, gregarine parasites. It was hypothesized that gregarine cysts were specific to the unique biochemistry (digestive tract enzymes) of the tunicate hosts (Ormières 1965). This does explain how overlapping distributions of a particular host and the dispersal of gregarine cysts into the water column could be specific, even though cysts from various gregarine species are likely taken up by the suspension-feeding tunicates haphazardly. A similar pattern of host specificity is also apparent in other gregarine groups such as *Selenidium* (from tube-forming polychaetes) (Schrével 1971), *Gregarina* (from insects) (Clopton et al. 1992), the Cephaloidophoridae (from crustaceans) (Perkins et al. 2000), and *Lithocystis* (from echinoderms) (Jangoux 1984), just to name a few.

The use molecular phylogenetics, specifically 18S rDNA, has supported many of these initial findings: gregarines infecting a particular host group are generally also closely related (Rueckert et al. 2011, 2015; Schrével et al. 2016; Wakeman and Leander 2013a, b). There are also some intriguing exceptions to this trend. Among marine gregarines, *Caliculium*, a parasite found in a hemichordate, branched among gregarines infecting terrestrial arthropods (Wakeman et al. 2014); and *Veloxidium*, *Pterospora*, and *Lithocystsis*, parasites of echinoderms, grouped with lecudinids infecting polychaetes, tunicates, and nemerteans (Wakeman and Leander 2012; Leander et al. 2006). To this end, establishing a catalogue of instances where gregarines have jumped and/or are shared among host groups, will be the first step in understanding the mechanisms and processes driving speciation and biodiversity of marine gregarines.

In the current study, we explore a situation where gregarines have 'jumped' between distantly related host groups, crustaceans and salps. *Cephaloidophora* cf. *flava* n. comb. (Ex. *Thalicola flava*) were collected from *Salpa fusiformis* Cuvier, 1804, and

a copepod, *Candacia bipinnata* Giesbrecht, 1889. A copepod was chosen for this work because cephaloidophorids have yet to be sequenced from a copepod host and having this data could be important for estimating the evolutionary history of this host-jumping event. Trophozoites and gamonts were processed for morphological analyses using light microscopy, as well as scanning and transmission electron microscopy, in order to compare newly generated data with that from previous work, and to make detailed observations that would help clarify the systematics of these gregarines. Because the vast majority of previous work done on this group is based on 18S rDNA, we also isolated single-cell isolates (or paired isolates in syzygy) for molecular analysis using the ribosomal operon.

Results

Trophozoites and gamonts of *Cephaloidophora* cf. *flava* n. comb. (Ex. *Thalicola flava*) were found in 32 out of 100 individuals of *Salpa fusiformis* (incidence = 32%). Trophozoites were bottle-shaped and had rounded posterior and anterior ends; the anterior being slightly narrowed (Fig. 1). A distinct protomerite was also seen in many individuals. Trophozoites had an average length of 432 lm (270–452 lm) and width of 163 lm (130–223 lm) ($n = 20$). A transverse septum was visible separating the protomerite and deutomerite. The nucleus was spherical, with an average diameter of 34 lm (32–46 lm), located in the deutomerite. Examples of gamonts joined in syzygy were also observed. These syzygy pairings consisted of a primite and 1 or 2 satellites. Satellites varied in size, most being smaller. Yet, satellites larger than the primite were observed (not photographed) (Fig. 1A–D). Gliding motility in both the trophozoite stages and gamonts was also observed. In order to confirm the origin of the parasite, photos were taken of the *C.* cf. *flava* n. comb. in the gut lumen of the salp (Fig. 1E, F). Although a number of copepods were observed within the tunic of the salp, *C.* cf. *flava* n. comb. was only observed attached to the inner wall of the gut lumen of *S. fusiformis*. Additional PCR screening of the 94 copepods taken from infected salp individuals, using primers specific to *C.* cf. *flava* n. comb, were negative.

Electron micrograph (SEM) images of the surface of *C.* cf. *flava* n. comb. were able to show the distinct portions of a gamont pairing (syzygy), including the epimerite, protomerite, and deutomerite of the primite, as well as a satellite that joined to the primite in a caudal-frontal syzygy orientation (Fig. 2). Transmission electron micrographs (TEM) through trophozoites and gamonts of this species highlighted the distribution of amylopectin and densely stained lipids; these starches and lipids were mainly observed in the deutomerite portion of the cell in mature trophozoites and gamonts (Fig. 3A). However, in less mature cells, the distribution appeared to be more uniform. Cross-sections of trophozoites appeared to show that there was a septum-like separation running longitudinally within the cell (Fig. 3B). The surface folds on the cell where dense and numerous (>100). Some folds were relatively shorter than others (Fig. 3D). On the apical ends of the cells, three-pointed, electron-dense 'rippled' structures adorned the apices of the folds. Radiations within the dense ripple structures were notably absent (Fig. 3E). The syzygy junction between a primate and satellite was also investigated. This region was found to contain a number of surface folds. Micronemes were clustered near the epimerite of the satellite (Fig. 3F).

Cephaloidophora bipinnatae n. sp. was observed in 17 of 100 specimens (incidence = 17%) of *Candacia bipinnata*. Trophozoite stages had an average length of 132 lm and width of 48 lm ($n = 15$) (Fig. 4A). A spherical nucleus with an average diameter of 10 lm ($n = 10$) was located in the deutomerite (posterior of the septa) (Figs 4A, 5C). Trophozoites and gamonts were cylindrical and sometimes appeared rounded. The posterior narrowed, and the anterior was rounded. The epimerite/protomerite region of the cell was less pronounced (Fig. 4C). The cell surface was covered with a dense number of surface folds (Fig. 4D). Transmission electron micrographs showed that there was a dense accumulation of lipids and amylopectin in the deutomerite (Fig. 5A, B), and a dense accumulation of surface folds was even around the circumference of the cell (Fig. 5B). Ultrastructural data also showed that the protomerite/epimerite region of the cell was highly reduced, while the deutomerite was more prominent (Fig. 5A, C, D). A septum was present in the cells, however, this septum was near the anterior end of the cell (Fig. 5D). Radiations and rippled structures were not observed at the apices of the surface folds (Fig. 5F).

The two novel 18S rDNA sequences generated from *C.* cf. *flava* n. comb. and *C. bipinnatae* n. sp. grouped with robust support within a clade comprised of gregarine apicomplexans isolated from

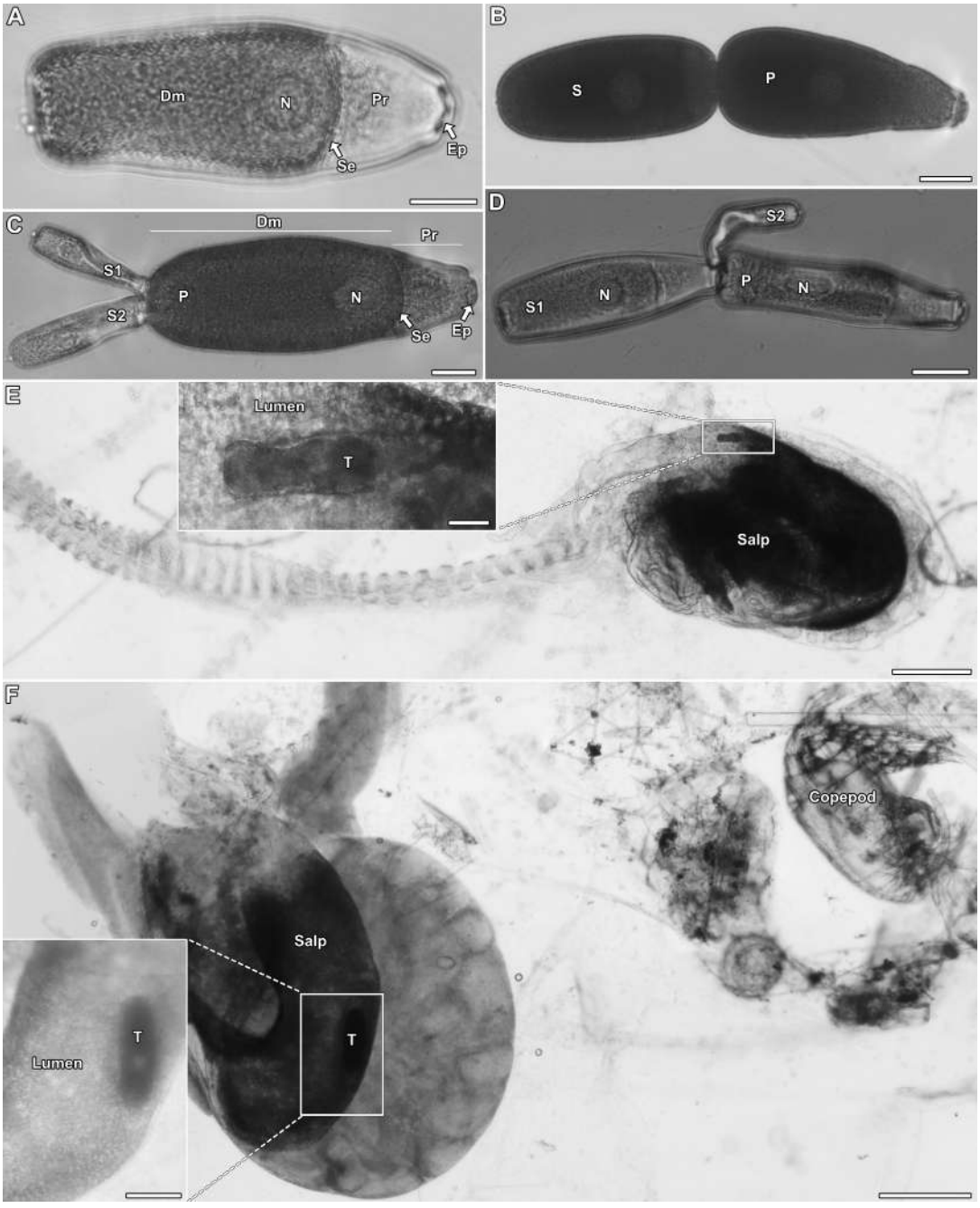

Figure 1. Light micrographs highlighting the general morphology of trophozoites and gamonts (in syzygy = sexual reproduction) of *Cephaloidophora* cf. *flava* n. comb within *Salpa fusiformis* (salp). **A.** Trophozoite showing the epimerite (Ep), protomerite (Pr) and deutomerite (Dm) separated by a transverse septum (Se), as well as the spherical nucleus (N) positioned within the deutomerite. **B.** Two gamonts joined in syzygy; the primite (P) and satellite (S) are joined in a caudo-frontal (head-to-tail) orientation (the epimerite of the primite is oriented towards the right). **C., D.** Examples of multiple gamonts associated in syzygy: each association consists of a primite (P) and two satellites (S1 and S2). Also observable are the epimerite regions (Ep), protomerite (Pr), deutomerite (Dm), and transverse septa (Se) as well as the nuclei (N). **E., F.** A trophozoite (T) in the gut lumen (Lumen) of *S. fusiformis*; **(inset)** high-magnification image of the trophozoite in the gut. A copepod (Copepod) is also visible within the salp. Scales: A–D = 50 lm; E = 500 lm (inset = 50 lm); F = 1 mm (inset = 100 lm).

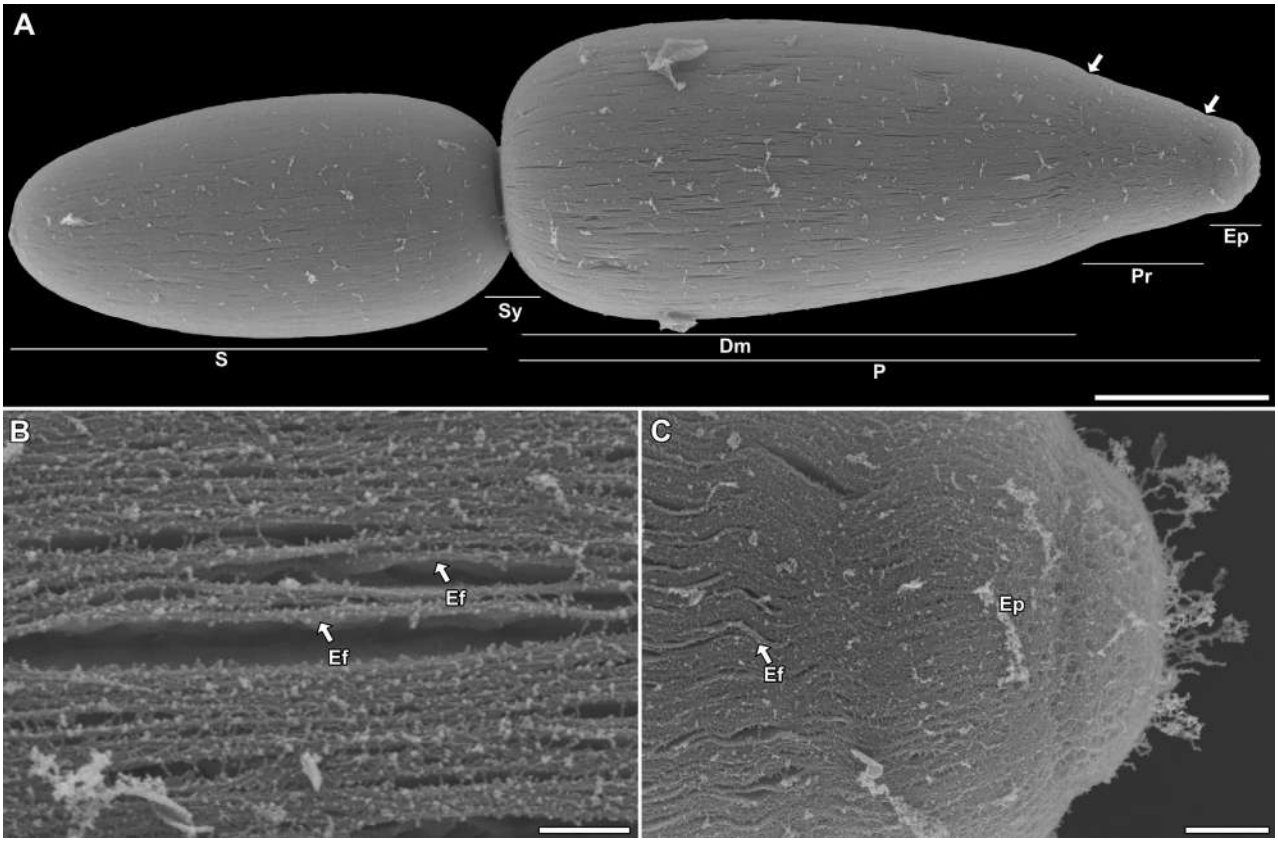

Figure 2. Scanning electron micrographs of *Cephaloidophora* cf. *flava* n. comb. **A.** Gamonts in syzygy showing the primite (P), satellite (S), epimerite (Ep), protomerite (Pr), and deutomerite (Dm), and the syzygy junction (Sy). Note that the anterior part of the primite has areas that appeared constricted (arrow) that correspond to the transverse septum separating the deutomerite, protomerite, and epimerite. **B.** High-magnification view of the epicytic folds (Ef) on the surface of the trophozoite. **C.** High-magnification image of the epimerite (Ep) covered in epicytic folds (Ef). Scales: A = 50 lm; B = 3 lm; C = 5 lm.

crustaceans (Fig. 6). Support for each of the main families within this clade (i.e., Cephaloidophoridae, Thiriotiidae, Ganymedidae, and Uradiophoridae) was high, with the exception of Ganymedidae, which had relatively low support. The new sequences from this study were within a clade, comprised of other cephaloidophorids. The relationships within this clade were not resolved (Fig. 6). Throughout the tree as a whole, bootstrap values were low. Higher support was typically only seen at nodes nearer the tips of the tree, compared to lower support at the nodes between the major lineages.

Analyses of the 18S rDNA dataset that focused on gregarines from crustaceans and affiliated environmental sequences did improve some of the internal node support within the clades representing the Cephaloidophoridae, Thiriotiidae, Ganymedidae, and Uradiophoridae; support between these clades, however, remained low (Fig. 7). The sequences from *C.* cf. *flava* n. comb. and *C. bipinnatae* n. sp. were nested within the Cephaloidophoridae, forming a clade, along with 10 environmental sequences, with moderate support (69ML/1.00PP). The novel sequences generated in this study grouped with robust support within environmental sequence clades with moderate support. Relationships between these subclades had only limited support (Fig. 7).

In the analyses where the 18S rDNA and 28S rDNA datasets were concatenated, *C.* cf. *flava* n. comb and *C. bipinnatae* n. sp. did branch as sister lineages, albeit with lower support (Supplementary Material Fig. S1). In this dataset, the gregarine from the salp and crustaceans were recovered as a monophyletic group on a long branch; internal nodes within this clade where not resolved. The backbone of this tree also garnered low support (Supplementary Material Fig. S1).

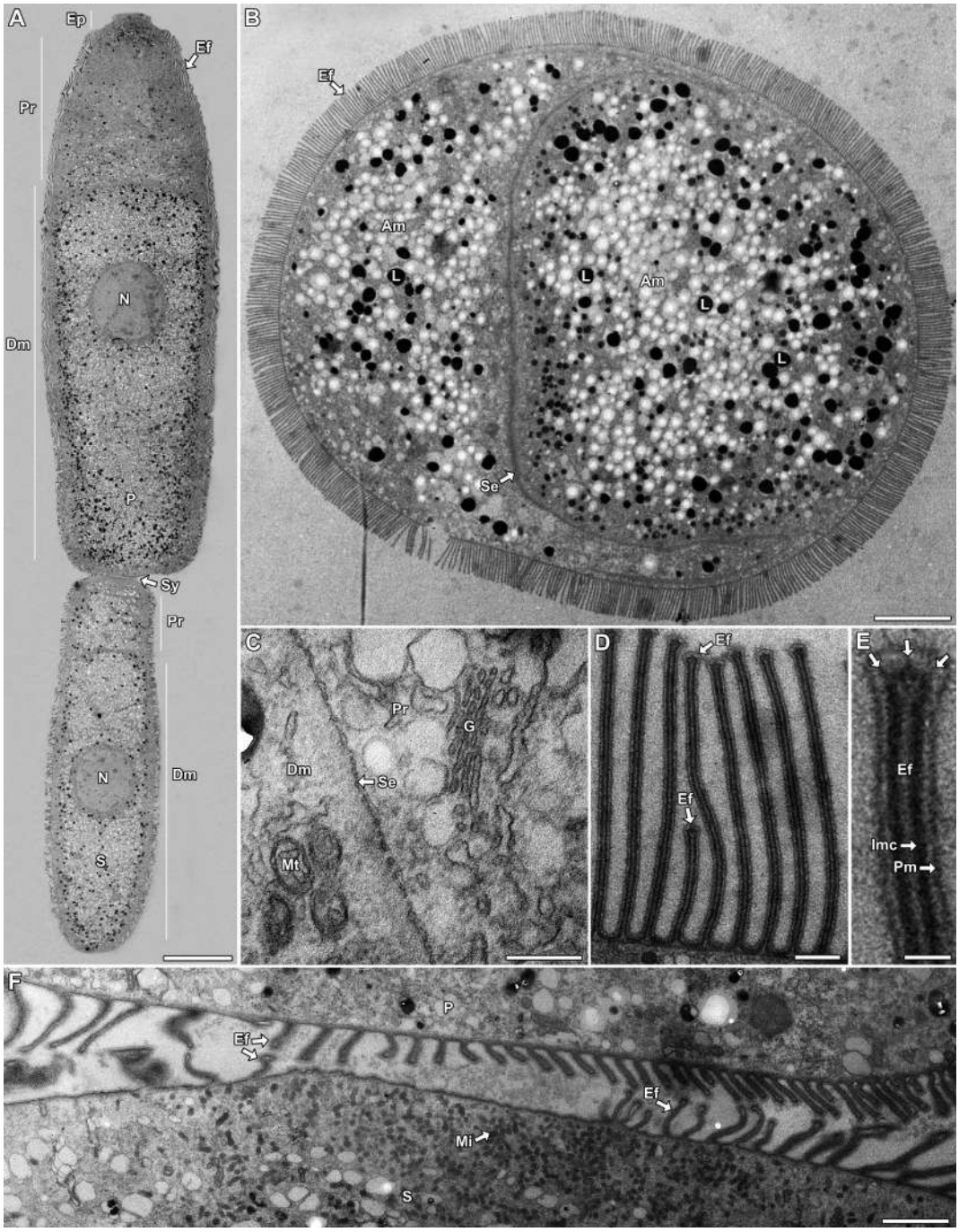

Figure 3. Transmission electron micrographs of *Cephaloidophora* cf. *flava* n. comb. **A.** Longitudinal section through gamonts in syzygy showing the primite (P) and satellite (S) and the point at which they are attached (Sy), as well as the epimerite (Ep), protomerite (Pr), deutomerite (Dm), epicytic folds (Ef) and nuclei (N). **B.** Cross-section through a trophozoite showing epicytic folds (Ef), amylopectin (=starch) granules (Am), electron-dense lipids (L), and a septum (Se) that transverses the section. **C.** High-magnification image through a longitudinal section showing the point at which the transverse septum (Se) divides the deutomerite (Dm) and protomerite (Pr). Also visible are mitochondria (Mt) and a Golgi apparatus (G). **D.** Cross-section showing the variable length of the epicytic folds (Ef). **E.** High-magnification cross section of an epicytic fold (Ef) showing the trilayer membrane comprised of the inner membrane complex (Imc) and plasma membrane (Pm). Note that the apex of the fold has rippled with three points (arrows), and the absence radial spokes in the apices. **F.** High-magnification image of the syzygy junction between the primite (P) and satellite (S). Also visible are micronemes (Mi) in the satellite, and epicytic folds (Ef). Scales: A = 10 lm; B = 5 lm; C = 200 nm; D = 300 nm; E = 100 nm; F = 500 nm.

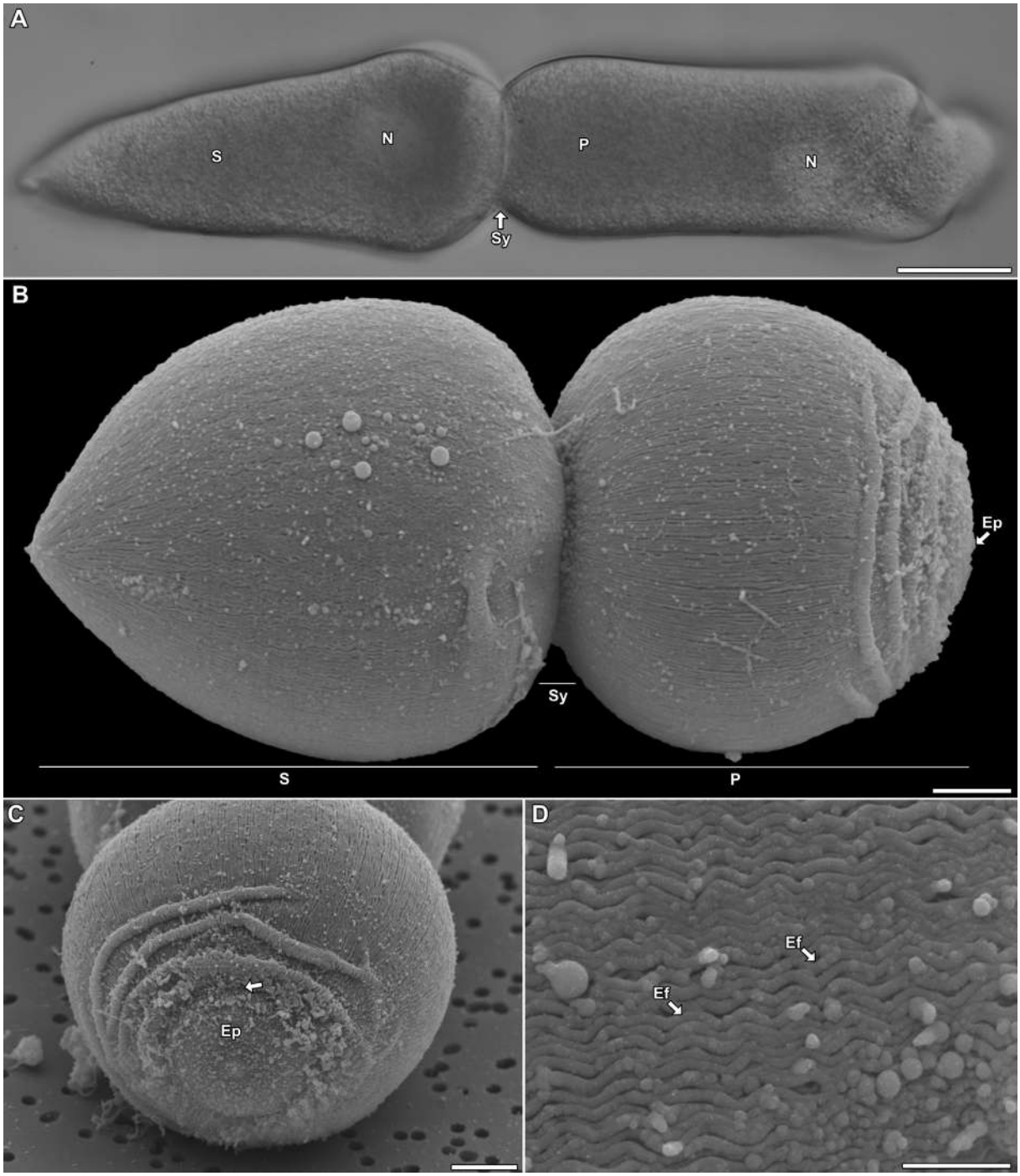

Figure 4. Light micrographs and scanning electron micrographs showing the general morphology of *Cephaloidophora bipinnatae* n. sp. **A.** Light micrograph of two gamonts in caudo-frontal (head-to-tail) syzygy. The point at which the primite (P) and satellite (S) are joined is denoted with "Sy"; the anterior epimerite is oriented to the right in the image; nuclei (N) are spherical. **B.** Scanning electron micrograph two gamonts (primite (P) and satellite (S)) in syzygy (Sy). The epimerite (Ep) appears folded. **C.** Electron micrograph of the Epimerite (Ep). Note the anterior region where the cell is constricted (arrow), forming the epimerite. **D.** High-magnification image of the trophozoite surface showing the epicytic folds (Ef). Scales: A = 20 lm; B = 10 lm; C = 5 lm; D = 2 lm.

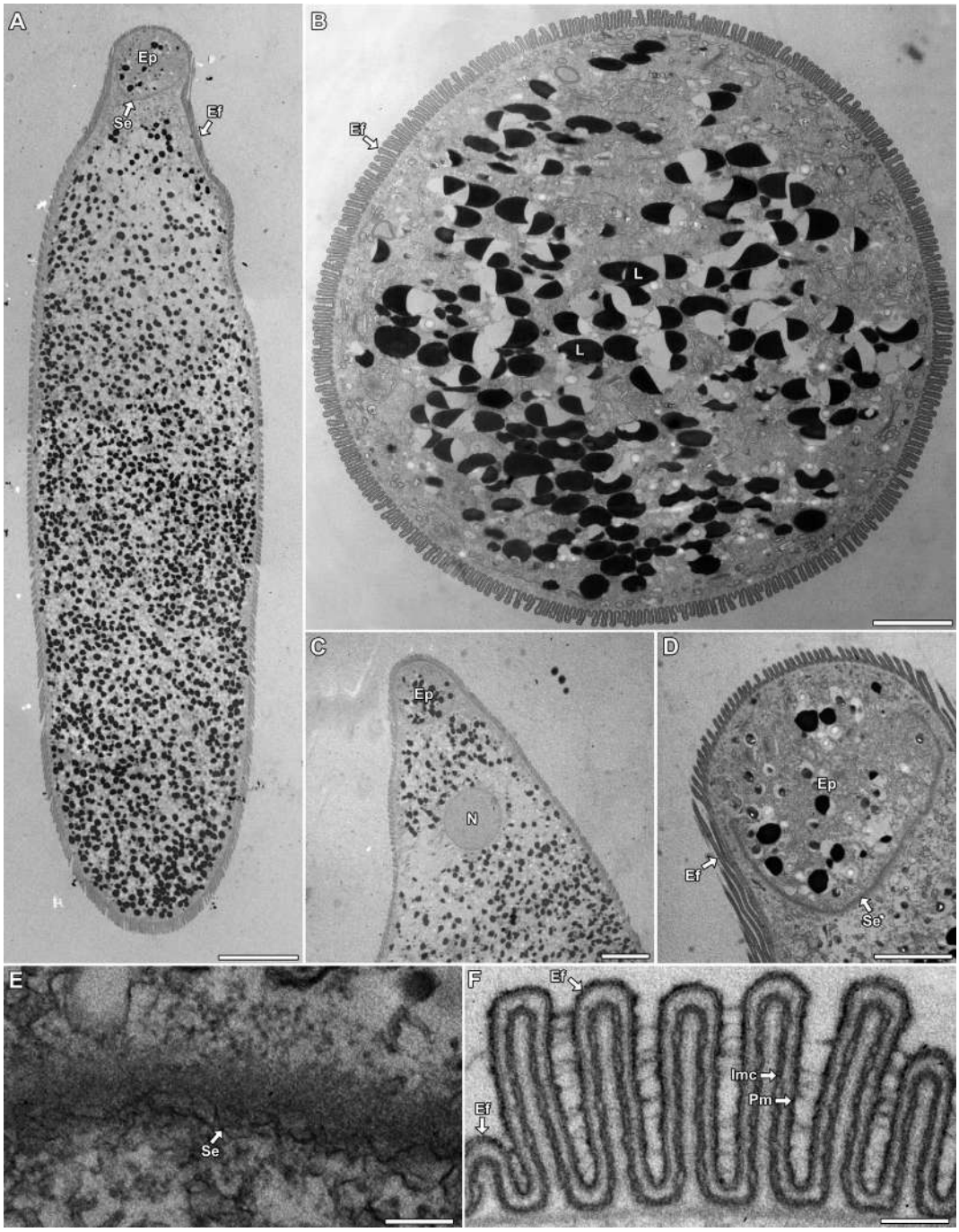

Figure 5. Transmission electron micrographs of trophozoite stages of *Cephaloidophora bipinnatae* n. sp. **A.** Longitudinal section showing the Epimerite (Ep) and the septum (Se) dividing it from the rest of the cell. Epicytic folds (Ef) are visible on the surface. **B.** Cross section through a trophozoite showing the pattern of epicytic folds (Ef), as well as the distribution of electron-dense lipids (L) throughout the cell. **C.** Tangential section through the anterior of a trophozoite showing the nucleus (N) relative to the epimerite (Ep). **D.** High-magnification longitudinal section of the epimerite (Ep) region showing the transverse septum (Se) and epicytic folds (Ef). **E.** High-magnification image of the transverse septum (Se). **F.** High-magnification image of the epicytic folds (Ef) showing the trilayer membrane comprised of the inner membrane complex (Imc) and plasma membrane (Pm). Note that ripple structures and radial spokes are not seen at the apices of the epicytic folds. Scales: A = 10 lm; B = 2 lm; C = 5 lm; D = 2 lm; E, F = 100 nm.

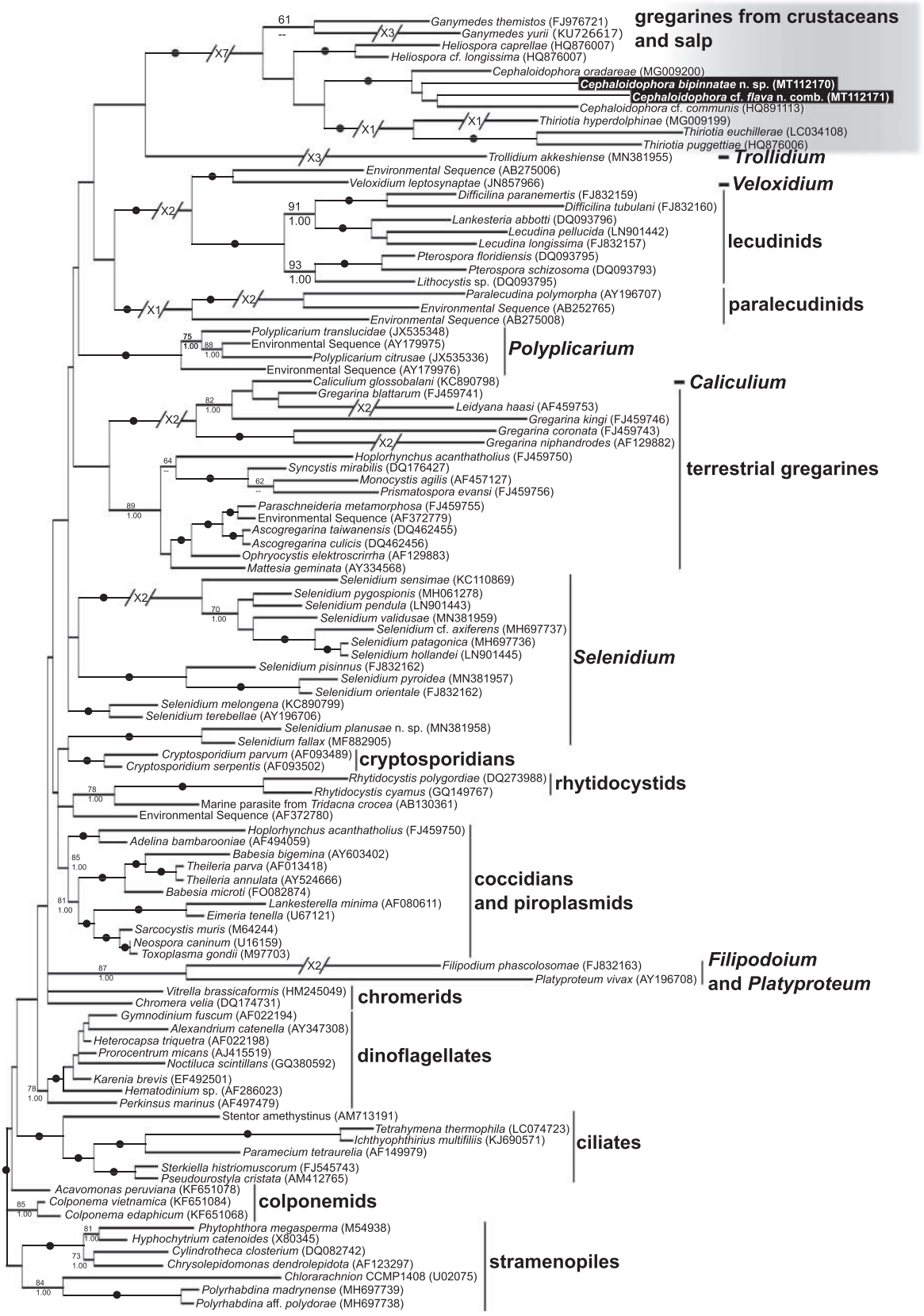
gregarines from crustaceans and salp
Ganymedes themistos (FJ976721)
Ganymedes yurii (KU726617)
Heliospora caprellae (HQ876007)
Heliospora cf. longissima (HQ876007)
Cephaloidophora oradareae (MG009200)
Cephaloidophora bipinnatae n. sp. (MT112170)
Cephaloidophora cf. flava n. comb. (MT112171)
Cephaloidophora cf. communis (HQ891113)
Thiriotia hyperdolphinae (MG009199)
Thiriotia euchillerae (LC034108)
Thiriotia puggettiae (HQ876006)
Trollidium akkeshiense (MN381955)
Trollidium
Environmental Sequence (AB275006)
Veloxidium leptosynaptae (JN857966)
Veloxidium
Difficilina paranemertis (FJ832159)
Difficilina tubulani (FJ832160)
Lankesteria abbotti (DQ093796)
Lecudina pellucida (LN901442)
Lecudina longissima (FJ832157)
lecudinids
Pterospora floridiensis (DQ093795)
Pterospora schizosoma (DQ093793)
Lithocystis sp. (DQ093795)
Paralecudina polymorpha (AY196707)
Environmental Sequence (AB252765)
Environmental Sequence (AB275008)
paralecudinids
Polyplicarium translucidae (JX535348)
Environmental Sequence (AY179975)
Polyplicarium citrusae (JX535336)
Environmental Sequence (AY179976)
Polyplicarium
Caliculum glossobalani (KC890798)
Caliculum
Gregarina blattarum (FJ459741)
Leidyana haasi (AF459753)
Gregarina kingi (FJ459746)
Gregarina coronata (FJ459743)
Gregarina niphandrodes (AF129882)
Hoplorhynchus acanthatholius (FJ459750)
Syncystis mirabilis (DQ176427)
Monocystis agilis (AF457127)
Prismatospora evansi (FJ459756)
Paraschneideria metamorphosa (FJ459755)
Environmental Sequence (AF372779)
Ascogregarina taiwanensis (DQ462455)
Ascogregarina culicis (DQ462456)
Ophryocystis elektroscrirrha (AF129883)
Mattesia geminata (AY334568)
terrestrial gregarines
Selenidium sensimae (KC110869)
Selenidium pygospionis (MH061278)
Selenidium pendula (LN901443)
Selenidium validusae (MN381959)
Selenidium cf. axiferens (MH697737)
Selenidium patagonica (MH697736)
Selenidium hollandei (LN901445)
Selenidium pisinnus (FJ832162)
Selenidium pyroidea (MN381957)
Selenidium orientale (FJ832162)
Selenidium melongena (KC890799)
Selenidium terebellae (AY196706)
Selenidium planusae n. sp. (MN381958)
Selenidium fallax (MF882905)
Selenidium
Cryptosporidium parvum (AF093489)
Cryptosporidium serpentis (AF093502)
cryptosporidians
Rhytidocystis polygordiae (DQ273988)
Rhytidocystis cyamus (GQ149767)
rhytidocystids
Marine parasite from Tridacna crocea (AB130361)
Environmental Sequence (AF372780)
Hoplorhynchus acanthatholius (FJ459750)
Adelina bambarooniae (AF494059)
Babesia bigemina (AY603402)
Theileria parva (AF013418)
Theileria annulata (AY524666)
Babesia microti (FO082874)
Lankesterella minima (AF080611)
Eimeria tenella (U67121)
Sarcocystis muris (M64244)
Neospora caninum (U16159)
Toxoplasma gondii (M97703)
coccidians and piroplasmids
Filipodium phascolosomae (FJ832163)
Platyproteum vivax (AY196708)
Filipodoium and Platyproteum
Vitrella brassicaformis (HM245049)
Chromera velia (DQ174731)
chromerids
Gymnodinium fuscum (AF022194)
Alexandrium catenella (AY347308)
Heterocapsa triquetra (AF022198)
Prorocentrum micans (AJ415519)
Noctiluca scintillans (GQ380592)
Karenia brevis (EF492501)
Hematodinium sp. (AF286023)
Perkinsus marinus (AF497479)
dinoflagellates
Stentor amethystinus (AM713191)
Tetrahymena thermophila (LC074723)
Ichthyophthirius multifiliis (KJ690571)
Paramecium tetraurelia (AF149979)
Sterkiella histriomuscorum (FJ545743)
Pseudourostyla cristata (AM412765)
ciliates
Acavomonas peruviana (KF651078)
Colponema vietnamica (KF651084)
Colponema edaphicum (KF651068)
colponemids
Phytophthora megasperma (M54938)
Hyphochytrium catenoides (X80345)
Cylindrotheca closterium (DQ082742)
Chrysolepidomonas dendrolepidota (AF123297)
Chlorarachnion CCMP1408 (U02075)
Polyrhabdina madrynense (MH697739)
Polyrhabdina aff. polydorae (MH697738)
stramenopiles

Discussion

Gregarines infecting salps: **Cephaloidophora *cf.* flava *n. comb.*** To date, three species of gregarines have been described from salps, all of which have been placed into the same genus, *Thalicola* Ormières, 1965 (Ormières 1965). These gregarines, *T. salpae* (Type), *T. ensiformis*, and *T. flava*, possess distinct septa, separating the protomerite and epimerite from the deutomerite portion of the cell. Septa are a feature that unites the Septatorina Lankester, 1885, a traditional grouping containing approximately 150 different gregarine genera, many of which infect terrestrial arthropods (e.g., the genus *Gregarina* in insects) (Perkins et al. 2000). In marine environments, the diversity of septatorid gregarines is much lower than that their terrestrial counterparts, and in this environment, they have only been described from crustaceans (Porosporidae Labbé, 1899, Cephaloidophoridae Kamm, 1922, Cephalolobidae Théodoridès and Desportes, 1975, and Uradiophoridae Grassé, 1953), and salps (*Thalicolidae* Théodoridès and Desportes, 1975) (Desportes and Schrével 2013a). The presence of septa in *Thalicola* is unique among gregarine parasites of tunicates and their relatives; in fact, all gregarine parasites from tunicates, with the exception of *Thalicola*, lack septa, and are grouped together into a single genus, *Lankesteria* Mingazzini, 1891 (Ormières 1965). It is likely due to these morphological differences, as well as habitat/host affinity, that the *Thalicola* was established because this group could not be reasonably combined with other aseptate *Lankesteria* from tunicates, and no available evidence could link *Thalicola* to the septate gregarines found in (marine) crustaceans or those of (terrestrial/aquatic) insects (Desportes and Schrével 2013a).

One of the main taxonomic conclusions of this study is to abolish *Thalicola* and move the three species of this group into the genus *Cephaloidophora*. The transferring of these three species into the *Cephaloidophora* is justified by similarities in their trophozoite/gamont morphology, as well as compelling evidence from molecular data. *Cephaloidophora cf. flava* n. comb. (Ex. *Thalicola flava*) was initially identified in this study based on morphological observations of trophozoite and gamont stages. This species is distinguished from other gregarines from salps based on the relative size of satellites compared to the primite, and a constriction of the epimerite/protomerite region which leads to the appearance of three distinct regions primite (or individual trophozoite): epimerite, a more bulbous protomerite, and deutomerite (Ormières 1965). Ormières (1965) did note the occurrence of gregarines in *S. fusiformis*, stating that they were similar to those gregarines (*T. salpae*) from *Salpa maxima* Forskål, 1775. However, due to lack of suitable material, no formal descriptions or material (photos or line drawings were made), and so direct comparison to our data is not possible. The geographic region (South Pacific) and host (*S. fusiformis*) represent new geographic and host ranges for *C.* cf. *flava* n. comb. (Ormières 1965; Wallis et al. 2017). However, we concluded not to erect a new species because there were limited morphological differences between previous work and observations in this study.

This is the first study to provide molecular data from gregarines from salps. The 18S rDNA sequence from *Cephaloidophora* cf. *flava* n. comb. grouped with robust support with other members of the Cephaloidophoroidea (i.e., gregarines infecting crabs, shrimp, amphipods, and copepods (Rueckert et al. 2011). In a more streamlined dataset that focused on this particular clade, *C.* cf. *flava* n. comb. grouped within the family Cephaloidophoridae. With this molecular result in mind, ultrastructural data (transmission electron micrographs) of *C.* cf. *flava* n. comb. were examined. Here, in addition to the septa, we also noted that axial structures were absent from the apices of the epicytic folds – another feature common to cephaloidophorids (Desportes et al. 1977).

Figure 6. Maximum-likelihood (ML) tree inferred from 18S rDNA sequences. Maximum-likelihood bootstrap values over 50 and Bayesian posterior probabilities (PP) over 0.95 are shown at the nodes (ML/PP). Black dots indicate statistical support of 95ML/0.99PP or higher. The scale bar represents inferred evolutionary distance in changes/site. The novel sequences from *Cephaloidophora* cf. *flava* n. comb. and *C. bipinnatae* n. sp. generated in this study are highlighted in bold font and black boxes. Some branches were shortened by multiples of the length of the substitutions/site scale bar (e.g., 1X).

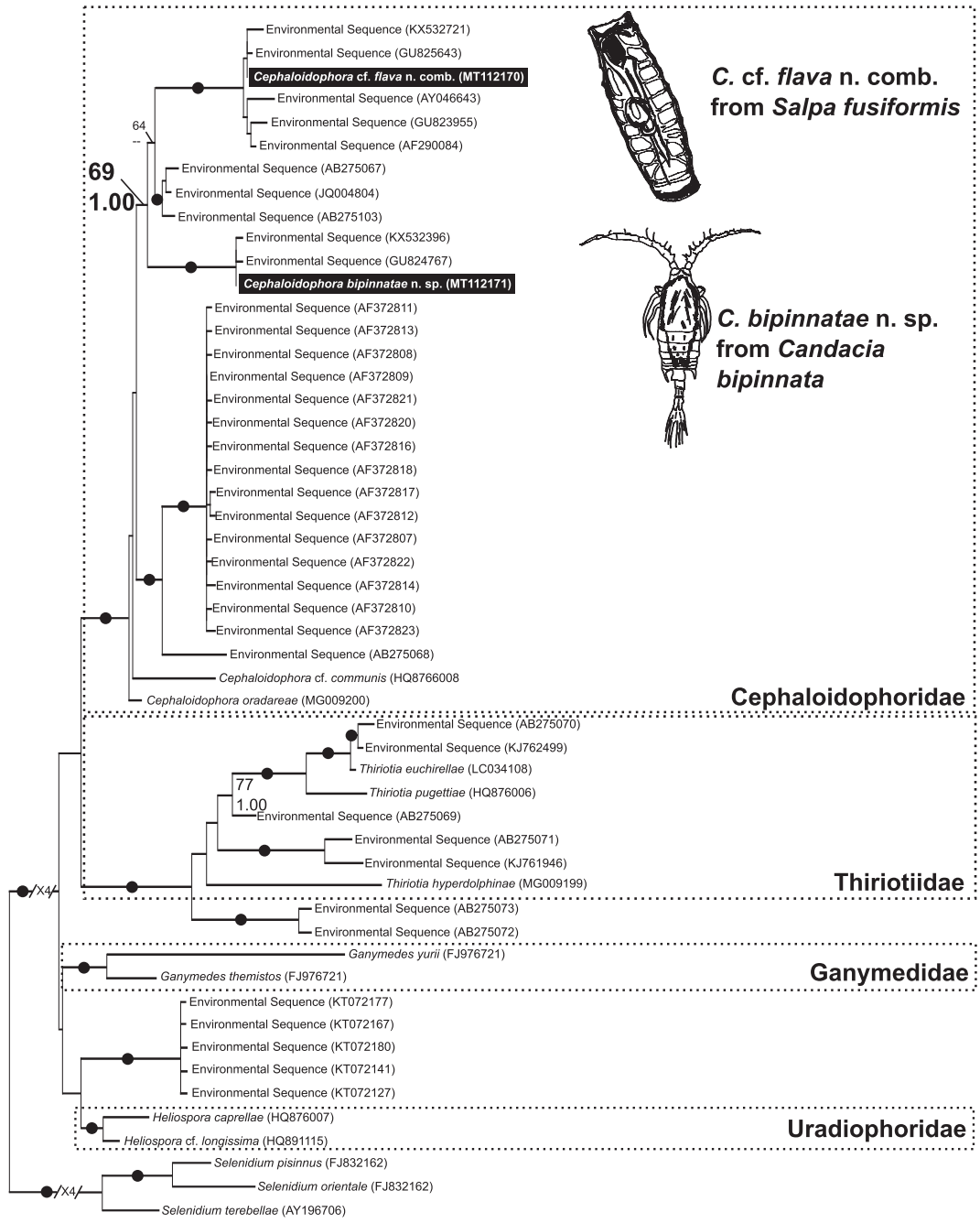

Figure 7. Maximum-likelihood (ML) tree inferred from 18S rDNA sequences along with environmental sequences from (probable) gregarines from crustaceans. Maximum-likelihood bootstrap values over 50 and Bayesian posterior probabilities 0.95 are shown at the nodes (ML/PP). Black dots indicate statistical support of 95ML/0.99PP or higher. The scale bar represents inferred evolutionary distance in changes/site. The novel sequences from *Cephaloidophora* cf. *flava* n. comb. and *C. bipinnatae* n. sp. generated in this study are highlighted in bold font and black boxes. Some branches were shortened by multiples of the length of the substitutions/site scale bar (e.g., 1X).

In an effort to build a more comprehensive molecular dataset that reflects recent efforts in the field (Paskerova et al. 2018; Wakeman 2020), the ITS and a large portion of the 28S rDNA were amplified. The resolution throughout these datasets (single-gene 28S rDNA, and a concatenated dataset with both 18S rDNA and 28S rDNA) was quite low, and many nodes were unresolved. This is likely due to

fast evolutionary rate of change along the ribosomal operon and the taxon sampling among these particular lineages. Gregarines are notorious for having long-branching ribosomal sequences. Septate gregarines (Leander et al. 2003), especially *Cephaloidophora* (Rueckert et al. 2011; Simdyanov et al. 2015), are some of the longest, even among gregarines. It's evident that the quick-evolving nature of the ribosomal operon will confound efforts to resolve some parts of the evolutionary history of gregarines.

Cephaloidophora *cf.* flava *n. comb. appears to be exclusive to* Salpa fusiformis. During the course of this study, we also examined copepods residing within the tunics of gregarine-infected salp, to check for the presence of gregarine parasites. Our photographic and molecular data suggested that these infections are exclusive to the salp. In this study, numerous (>200) copepods were found within infected salp and dissected for gregarines, none appeared to be infected with any type of gregarine. In case we overlooked infections, or were missing cryptic life stages, we also attempted to amplify the 18S rDNA of *C.* cf. *flava* n. comb., using specific primers and genomic DNA extracted from 94 of these copepods; all were negative. Previous studies also never reported finding these gregarines in the copepods. Although, absence is challenging to definitely prove, what can be said is that the presence of *C.* cf. *flava* n. comb. in this salp is more common than in the associated copepods, if they exist at all.

Gregarines infecting calanoid copepods:* Cephaloidophora bipinnatae *n. sp. In this study, we also establish a new gregarine species, *Cephaloidophora bipinnatae* n. sp., from the calanoid copepod *Candacia bipinnata*. Three gregarine species have been reported from copepods, *Cephaloidophora petiti* Gobillard, 1964 (host species: *Candacia longimana* Claus, 1853), *Ganymedes apsteini* Théodoridès and Desportes, 1972 (host species: *Calanus finmarchicus* Gunnerus, 1770), and *Thiriotia euchirellae* Sano et al. 2016 (host species: *Euchirella* rostrate Claus, 1866); molecular data is only available for *T. euchirellae* (Gobillard 1964; Sano et al. 2016; Théodoridès and Desportes 1972). *Cephaloidophora bipinnatae* n. sp. shares a number of features with other members of the *Cephaloidophora* including a transverse septum and rounded epimerite/mucron. It can therefore be distinguished morphologically from both *Ganymedes* which processes a globular or sucker-like mucron, and *Thiriotia* which is more elongate (Desportes and Schrével 2013a). Molecular data generated from *C. bipinnatae* n. sp. was congruent with these morphological observations and branched within the Cephaloidophidae.

In comparison to the trophozoites of *Cephaloidophora petiti* described from the congeners *Candacia longimana* Claus, 1853 and *C. aethiopica* Dana, 1848, trophozoites of *C. bipinnatae* n. sp. were almost double in length and width. The trophozoites of *C. bipinnatae* n. sp., had pointed posterior ends, compared to the rounded ends of *C. petiti* (Gobillard 1964). Additionally, the protomerite/epimerite region in *C. bipinnatae* n. sp. contains a discrete septum, making the anterior regions of the cell (protomerite/epimerite) difficult to discern under a light microscope; these regions in *C. petiti* are more pronounced, and a septum is clearly visible with a light microscope (Gobillard 1964). Considering these morphological differences, host affinity, and the vast geographic distances separating the type localities of *C. petiti* and *C. bipinnatae* n. sp. (*C. petiti* was described from the French Mediterranean), it is our conclusion that new species should be erected to encompass this diversity (summary of traits in Supplementary Material Table S2). Molecular data would be useful in this situation to further decipher the diversity of gregarines infecting pelagic copepods.

***Cephaloidophorid gregarines in salp: impacts on molecular ecology and evolutionary scenarios*.** One of the more surprising results from this study was the molecular phylogenetic position of *Cephaloidophora* cf. *flava* n. comb. within a clade that, until now, was thought to exclusively contain gregarines that parasitize crustaceans (Rueckert et al. 2011). An important aspect of these results pertains to the field of molecular ecology. Prior to the current study, any environmental sequence data branching among the Cephaloidophoridae would have been most likely attributed to parasites of crustaceans, not salps. In this way, the results from this study aid in the ability to more accurately assess environmental sequence data. Salps (as well as copepods) are major contributors to global pelagic ecosystems (Ishak et al. 2017). Inherently, a better understanding of the parasites with which they associate is also of significance.

Nevertheless, understanding the exact scenario (s) that led to this "jump" is unclear. It is evolutionarily simpler to conclude that these gregarines moved from a crustacean host to a salp because the over-

whelming majority of sequences in this clade come from gregarines infecting crustaceans, and the sequences from *C.* cf. *flava* n. comb are not early branching within this clade. Under this hypothesis, there are different avenues by which this could have happened. The molecular data we gathered does support, to a certain degree, a copepod origin for the cephaloidophorid infection in salps. The 18S rDNA from the *C. bipinnatae* n. sp. infecting free-living *Candacia bipinnata* in this study did branch sister to those of *C.* cf. *flava* n. comb., albeit with moderate support.

Expanding on this copepod-origin scenario, the gregarines in salps could have conceivably originated from a free-living or symbiotic relationship with a copepod. Salps are known to be prolific grazers of ocean plankton communities (Ishak et al. 2017). It is logical to think that gregarine cysts from cephaloidophorids (measuring approximately 20 lm –30 lm) (Hoshide 1969) could, and are, regularly filtered through salps as they feed (Harbison and McAlister 1979). It is noteworthy that *Candacia* feed on appendicularians, and *Euchirella* feeds on appendicularian houses (Ohtsuka and Nishida 1997). Some copepods, and other crustaceans such as hyperiid amphipods, live within the tunics of salps (Heron 1973; Madin and Harbison 1977); some of these crustaceans are parasites and others act as predators. However, while it is conceivable that a long-term and consistent association between copepods and salps resulted in a host-jumping event of their gregarine parasites, the results of our molecular phylogenetic datasets are not definitive, and as more data is collected, a different hypothesis to describe this diversity could emerge. Additionally, the occurrence of cephaloidophids in other salp species in distant geographic locations including the Southern Ocean (Wallis et al. 2017) and Mediterranean (Ormières 1965) suggests that these infections are not endemic to salps in the South Pacific but are global in their distribution. A broader sampling scheme with more molecular data from salps and their gregarine parasites would be needed to address whether these infections have occurred multiple times independently between crustaceans and salps, or whether this 'jump' was a singular event and the diversity of gregarines within salps is a result of subsequent radiations.

Taxonomic Summary

Phylum: Myzozoa Cavalier-Smith and Chao, 2004
Subphylum: Apicomplexa Levine, 1970
Order: Eugregarinorida, Léger, 1900

Remarks We propose to abolish the genus *Thalicola*, and transfer the three species in this genus, *T. salpae*, *T. ensiformis*, and *T. flava*) into the genus *Cephaloidophora.*

Family Cephaloidophoridae Kamm, 1922
Genus *Cephaloidophora* Mavrodiadi, 1908

Cephaloidophora cf. *flava* n. comb. Roboz, 1886; Ormières, 1965 emend. Wakeman, Hiruta, Kondo, Ohtsuka 2020 (Basionym *Thalicolia flava* Roboz, 1886; Ormières, 1965)

Description Trophozoites elongate; bottle-shaped. Average length 432 lm; average width 163 lm. Portions of trophozoites and gamonts divided by septum, forming protomerite and deutomerite. Cells circular in cross section with numerous (hundreds) of epicytic surface folds; surface folds with three-pointed, electron-dense 'rippled' structures near apices; radiations absent within apices. Nucleus spherical with average diameter of 34 lm. Trophozoites lacked obvious epicytic folds on the surface. Epimerite and posterior rounded. Syzygy caudo-frontal, often with multiple satellites connected to a primite. Satellites sometimes larger than primite. Movement by gliding motility. Amylopectin localized to deutomerite in mature trophozoites; uniformly distributed in immature gamonts.

DNA sequence ribosomal sequence data has been deposited into NCBI (GenBank MT112170).

Locality West Pacific (31°03′9.71″n 131°38′3.03″ E). Pelagic host abundantly found using an ORI-net at a depth of ~1000 m.

Type habitat Marine

Host *Salpa fusiformis* Cuvier, 1804 (Chordata, Thaliacea, Salpidae)

Location in host Intestinal lumen

Iconotype Figure 1A

Hapantotype Trophozoites on SEM stubs with a gold sputter coat have been stored in the algal and protist collection in the Hokkaido University Museum (KCW_Cephaloidophora_cf_flava_1).

LSID 14783a9a-eae3-4e2b-bc59-b9206ca8dfcb

Cephaloidophora bipinnatae n. sp. wakeman, hiruta, kondo, ohtsuka, 2020

Description Trophozoites elongate or slightly pudgy appearance. Average length 132 lm; average width 48 lm. Portions of trophozoites and gamonts divided by septum, forming protomerite and deutomerite. Septum discrete, forming shallow, discrete protomerite (epimerite). Cells circular in cross sec-

tion with numerous (hundreds) of epicytic surface folds; surface folds lacking ripples near apices; radiations absent within the apices. Nucleus spherical with average diameter of 10 lm. Epimerite rounded and slightly at times slightly narrowed; posterior narrowed to a point. Syzygy caudo-frontal; multiple satellites not observed. Movement by gliding motility. Amylopectin and dense lipids observed throughout deutomerite.

DNA sequence ribosomal sequence data has been deposited into NCBI (GenBank MT112171).

Type Locality West Pacific (33°50′4.20″n 136°54′3.30″E). Pelagic host commonly found using an ORI-net at a depth of ~1000 m.

Type habitat Marine

Type Host *Candacia bipinnata* Giesbrecht, 1889 (Arthropoda, Crustacea, Copepoda)

Location in host Intestinal lumen

Iconotype Figure 4A

Hapantotype Trophozoites on SEM stubs with a gold sputter coat have been stored in the algal and protist collection in the Hokkaido University Museum (KCW_Cephaloidophora_bipinnatae_1).

LSID 14783a9a-eae3-4e2b-bc59-b9206ca8dfcb

Etymology the species name, *bipinnatae*, refers to the host species from which this cephaloidophorid parasite was isolated.

Methods

Collection of hosts and isolation of parasites: *Salpa fusiformis* was collected from the Southwest Pacific Ocean on November 2, 2019 aboard TRV TOYOSHIO MARU. *Candacia bipinnata* was collected November 27, 2018 aboard TRV SEISUI MARU. Salp and copepod samples were collected using an ORI-net (Omori et al. 1965) at a depth between 1000–1100 m from coordinates 31° 03′9.71″N, 131°38′3.03″E and 33°50′4.20″N, 136° 54′3.30″E, respectively. Host organisms were held in cool seawater (on ice), prior to dissection. Their digestive tracts were dissected out using fine forceps. One-hundred individuals of each host species were examined for apicomplexan infections. Feeding stages (trophozoites), and paired gamonts (syzygy) were isolated using hand-drawn glass pipettes, and subsequently washed in filtered, autoclaved seawater until clean for further morphological and molecular analysis. In addition to the free-living *C. bipinnata*, copepods (>200) present within the tunics of *S. fusiformis* were also examined for gregarine infections. Ninety-four of these copepods, isolated from 10 different infected salp, were fixed in 100% ethanol for subsequent molecular work.

Light microscopy, scanning electron microscopy and transmission electron microscopy: Light micrograph images and videos were taken using an Olympus CKX53 (Tokyo, Japan) inverted microscope connected to a Canon EOS Kiss X9i camera (Tokyo, Japan). For scanning electron microscopy, individuals were transferred to a 3–5 lm mesh filter in 2.5% glutaraldehyde in seawater and held on ice for 15 min. After washing the samples three times (5 min each) in seawater, 1% OsO_4 was placed on the samples for 30 min. The samples were subsequently washed with distilled water and dehydrated through a graded series of ethanol (30%, 50%, 75%, 80%, and 100%) for 5 min at each step. Samples were critical point dried with CO_2, sputter-coated with 5 nm gold and viewed using a Hitachi N-3000 (Tokyo, Japan) SEM. For transmission electron microscopy, individual cells were fixed in 2.5% glutaraldehyde in seawater on ice for 30 min, washed in seawater, and post fixed with 1% OsO_4 on ice for 1.5 hours; both fixation steps were performed in the dark. Following the fixation with OsO_4, samples were washed in seawater, and dehydrated through a graded series of ethanol (30%, 50%, 75%, 80%, and 100%) for 5 min at each step, and subsequently moved to a 1:1 acetone/ethanol mixture, and a 100% acetone solution for 10 min each. Samples were then placed in a 1:1 resin (Agar Low Viscosity Resin, Agar Sciences)/acetone mixture for 30 min, followed by 100% resin overnight at room temperature. Resin was exchanged the following day, and samples were polymerized at 68 °C for 32 hours. Samples were cut with a diamond knife and viewed with a Hitachi-7400 (Tokyo, Japan) TEM.

DNA extraction, PCR amplification, and sequencing: Single-cell isolates of each parasite were placed in 0.2 ml PCR tubes. Total genomic DNA was extracted following the manufacturers protocol using a FFPE DNA extraction kit (Lucigen, Wisconsin, USA). The primers PF1 and SSUR4, were initially used to amplify 18S rDNA using the following protocol on a thermal cycler: Initial denaturation 95 °C 5:00 min; 35 cycles of 95 °C 0:30 s, 52 °C 0:30 s, 72 °C 2:00 min; final extension 72 °C 7:00 min. Subsequently, 1 ll of the initial PCR relation was used in a second PCR with PF1-CrustR and CrustF-SSUR4 under the following parameters:

Initial denaturation 95 °C 5:00 min; 25 cycles of 95 °C 0:30 s, 52 °C 0:30 s, 72 °C 1:40 min; final extension 72 °C 7:00 min. To amplify 28S rDNA sequences, the primers Salp1700F (or Crust1700F)-LSU3000R were used in an initial PCR to amplify the ITS regions as well as 28S rDNA using the following program on a thermocycler: 95 °C 5:00 min; 25 cycles of 95 °C 0:30 s, 52 °C 0:30 s, 72 °C 3:00 min; final extension 72 °C 7:00 min. Subsequently, 1 ll of these initial PCR reactions were used in a second round of amplifications using the primer pairs 25R1-Salp1700F (or Crust1700F), 25F1-LSU R2, and LSU2200F-LSU3000R, and LSU D3A-LSU3000R following the program on a thermocycler: Initial denaturation 95 °C 5:00 min; 25 cycles of 95 °C 0:30 s, 52 °C 0:30 s, 72 °C 1:50 min; final extension 72 °C 7:00 min. In each PCR reaction, Econotaq 2X Mastermix (Lucigen, Middleton, USA) was used, following the manufacturer's protocols. PCR products were purified using a Qiagen PCR purification kit (Qiagen, Germantown, USA); 1 μl of purified product was used in a sequencing reaction with ABI BigDye Terminator v1.1 (Applied Biosystems, Massachusetts, USA) and subsequently purified with ethanol, before being eluted in 18 μl Hi-Di Formamide (Applied Biosystems, Massachusetts, USA) and sequenced on a 3130 Genetic Analyzer (Applied Biosystems, Massachusetts, USA). The novel sequences generated in this study were deposited in NCBI's GenBank (MT112170-MT112171). All primers used in this study are listed in Supplementary Material Table S1.

In the case of the 94 copepods that were isolated from the infected salp and fixed in 100% ethanol, individuals were dried and placed in 1.5 ml Eppendorf tubes. Sterile pestles were used to crush the copepods. Total genomic DNA was then extracted using a DNeasy Blood and Tissue Kit, following the manufacturers protocols. Samples were screened using the nested PCR protocol described above for the 18S rDNA (PF1 + CrustR and CrustF + SSUR4) of *Cephaloidophora* cf. *flava* n. comb. A positive control (DNA extracted from a single-cell isolate of *C.* cf. *flava* n. comb. fixed in 100% ethanol using the DNeasy Blood and Tissue Kit) was also used to decrease the likelihood of a false negative.

Phylogenetic analyses: New sequences generated in this study were identified by BLAST. Three molecular phylogenetic datasets were generated and viewed using Mesquite 3.6 (Maddison and Maddison 2015): 1) an 18S rDNA alignment (124 taxa); 2) a 28S rDNA alignment (63 taxa); and 3) a concatenated 18S + 28S rDNA alignment (58 taxa). MUSCLE (Edgar 2004) was used under the default settings to align all datasets used for phylogenetic analyses. The alignment was trimmed with Gblocks (Castresana 2000; Talavera and Castresana 2007), only selecting for allowing gaps within the final blocks. final alignments used for phylogenetic analyses included 1254, 2672, and 4277 bp for 18S rDNA, 28S rDNA, and the concatenated datasets, respectively.

The best-fit model for each dataset was selected using IQ-TREE under AICc (Trifinopoulos et al. 2016). Maximum-likelihood (non-parametric bootstrap) analyses on the three datasets were subsequently run with IQ-TREE using GTR + F + R10; GTR + F + R10, and GTR + F + R6, as the model of evolution for the 18S rDNA, 28S rDNA, and the concatenated 18S + 28S rDNA datasets, respectively; each analysis ran for 500 bootstrap pseudoreplicates.

All Bayesian analyses were performed using the program MrBayes 3.2.5 (Ronquist and Huelsenbeck 2003). The program was set to operate with GTR + I + G, and four Monte Carlo Markov Chains (MCMC) starting from a random tree. A total of 7,000,000, 7,500,000 and 170,000,000 runs were completed for 18S, 28S and concatenated (18S + 28S rDNA) datasets, respectively. Generations were calculated with trees sampled every 100 generations and the first 70,000, 75,000 and 1,700,000 trees in each run were discarded as burn-in. When the standard deviation of split frequencies fell below 0.01, the program was set to terminate. Posterior probabilities correspond to the frequency at which a given node was found in the post-burn-in trees.

Declaration of Competing Interest

The authors declare that they have no known competing financial interests or personal relationships that could have appeared to influence the work reported in this paper.

Acknowledgements

This work was supported by Japanese Society for the Promotion of Science (JSPS) grants 18K14774 and PG6R180004 to KCW; additional funds and administrative support were provided to KCW by the Institute for the Advancement of Higher Education at Hokkaido University. Samples were collected with the kind support and assistance by the crew of TSV SEI-

SUI MARU (Mie University) and TSV TOYOSHIO MARU (Hiroshima University). Support for the critical point drying of samples and access to a critical point dryer was provided by the Research Faculty of Agriculture, Hokkaido University. We would like to especially thank Joseph Schrével for thoughtfully providing literature sources for our reference, as well as reviewers of this manuscript for their comments and suggestions.

Appendix A. Supplementary Data

Supplementary data to this article can be found online at https://doi.org/10.1016/j.protis.2021.125822.

References

Adl SM, Bass D, Lane CE, Lukeš J, Schoch CL, et al. (2019) Revisions to the classification, nomenclature, and diversity of eukaryotes. J Eukaryot Microbiol **66**:4–119

Castresana J (2000) Selection of conserved blocks from multiple alignments for their use in phylogenetic analysis. Mol Biol Evol **17**:540–552

Clopton RE, Percival TJ, Janovy J (1992) Host stadium specificity in the gregarine assemblage parasitizing *Tenebrio molitor*. J Parasitol **78**:334–337

Desportes I, Schrével J (2013a). Treatise on Zoology—Anatomy, Taxonomy, Biology: The Gregarines: Early Branching Apicomplexa, vol. 1. Brill Publ, Leiden, Netherlands, 1-376

Desportes I, Schrével J (2013b). Treatise on Zoology—Anatomy, Taxonomy, Biology: The Gregarines: Early Branching Apicomplexa, vol. 2. Brill Publ, Leiden, Netherlands, 377-710

Desportes I, Vivarès CP, Théodoridès J (1977) Intérêt taxinomique de l'ultrastructure épicytaire chez *Ganymedes* Huxley, *Porospora* Schneider et *Thiriotia* n.g. Eugrégarines parasites de Crustacés. Ann Sci Nat Zool 12 Ser **19**:261–277

Edgar RC (2004) MUSCLE: multiple sequence alignment with high accuracy and high throughput. Nucleic Acid Res **35**:1792–1797

Gobillard M-O (1964) *Cephaloidophora petiti* sp. n. grégarine parasite de copépods pélagiques de la région de Banyuls (note préliminaire). Vie et Milieu Suppl **17**:107–113

Grassé P-P (1953) Classe de Grégarinomorphes. In Grassé P-P (ed) Traité De Zoologie. Anatomie, Systématique, Biologie. Masson, Paris, pp 550–690

Harbison GR, McAlister VL (1979) The filter-feeding rates and particle retention efficiencies of three species of *Cyclosalpa* (Tunicata, Thaliacea). Limnol Oceanogr **24**:875–892

Heron AC (1973) A specialized predator-prey relationship between the copepod *Sapphirina angusta* and the pelagic tunicate *Thalia democratica*. J Mar Biol Ass UK **53**:429–435

Hoshide K (1969) Studies on gregarines from Japan I. *Cephaloidophora warekara* n. sp. and two other gregarines from crustaceans. J Fac Sci Hokkaido Univ Ser VI Zool **17**:6–16

Ishak ANH, Clementson LA, Eriksen RS, van den Enden RL, Williams GD, Swadling KM (2017) Gut contents and isotopic profiles of *Salpa fusiformis* and *Thalia democratica*. Mar Biol **164**:144–154

Jangoux M (1984) Diseases of echinoderms. Helgol Meeresunters **37**:207–216

Kristmundsson Á, Erlingsdóttir Á, Freeman M (2015) Is an apicomplexan parasite responsible for the collapse of the Iceland scallop (*Chlamys islandica*) stock? PLoS ONE **10 (12)**: e0144685

Leander BS (2008) Marine gregarines – evolutionary prelude to the apicomplexan radiation? Trends Parasitol **24**:60–67

Leander BS, Clopton RE, Keeling PJ (2003) Phylogeny of gregarines (Apicomplexa) as inferred from small-subunit rDNA and beta-tubulin. Int J Syst Evol Microbiol **53**:345–354

Leander BS, Lloyd SAJ, Marshall W, Landers SC (2006) Phylogeny of marine gregarines (Apicomplexa)—*Pterospora*, *Lithocystis*, and *Lankesteria*—and the origin(s) of coelomic parasitism. Protist **157**:45–60

Maddison WP, Maddison DR (2015) Mesquite: a modular system for evolutionary analysis. Version 3.04 http://mesquiteproject.org.

Madin LP, Harbison GR (1977) The association of Amphipoda Hyperiidea with gelatinous zooplankton. I. Associations with Salpidae. Deep Sea Res **24**:449–463

Moore RB, Oborník M, Janouškovec J, Tomáš Chrudimský, Marie Vancová, Green DH, Wright SW, Davies NW, Bolch CJS, Heimann K, Šlapeta J, Hoegh-Guldberg O, Logsdon JM, Carter D (2008) A photosynthetic alveolate closely related to apicomlexan parasites. Nature **451**:959–963

Morrison DA (2009) Evolution of the Apicomplexa: where are we now? Trends Parasitol **25**:375–382

Ohtsuka S, Nishida S (1997) Reconsideration of feeding habits of marine pelagic copepods (Crustacea). Ocean Japan **6**:299–320

Omori M, Marumo R, Aizawa Y (1965) A 160-cm opening-closing plankton net. J Ocean Soc Japan **21**:245–252

Ormières R (1965) Recherches sur les Sporozoaires parasites des Tuniciers. Vie et Milieu **15**:823–946

Perkins FO, Barta JR, Clopton RE, Pierce MA, Upton SJ (2000) Phylum Apicomplexa. In Lee JJ, Leedale GF, Bradbury P (eds) The Illustrated Guide to the Protozoa. 2nd edn. Allen Press Inc; Lawrence, pp. 190–304

Paskerova GG, Miroliubova TS, Diakin A, Kováčiková M, Valigurová A, Guillou L, Aleoshin VV, Simdyanov TG (2018) Fine structure and molecular phylogenetic position of two marine gregarines, *Selenidium pygospionis* sp. n. and *S. pherusae* sp. n., with notes on the phylogeny of Archigregarinida (Apicomplexa). Protist **169**:826–852

Ronquist F, Huelsenbeck JP (2003) MrBayes 3: Bayesian phylogenetic inference under mixed models. Bioinformatics **19**:1572–1574

Rueckert S, Simdyanov TG, Aleoshin VV, Leander BS (2011) Identification of a divergent environmental DNA sequence clade using the phylogeny of gregarine parasites (Apicomplexa) from crustacean hosts. PLoS ONE **6(3)**: e18163

Rueckert S, Wakeman KC, Jenke-Kodama H, Leander BS (2015) Molecular systematics of marine gregarine apicomplexans from Pacific tunicates, with descriptions of five novel species of *Lankesteria*. Int J Syst Evol Microbiol **65**:2598–2614

Sano M, Miyamoto H, Nishida S (2016) *Thiriotia euchirellae* n. sp., a new gregarine species (Apicomplexa: Eugregarinorida) from the mesopelagic copepod *Euchirella rostrata* in Sagami Bay, Japan. Mar Biodiv **46**:753–760

Simdyanov TG, Diakin AY, Aleoshin VV (2015) Ultrastructure and 28S rDNA phylogeny of two gregarines: *Cephaloidophora* cf. *communis* and *Heliospora* cf. *longissima* with remarks on gregarine morphology and phylogenetic analysis. Acta Protozool **54**:241–263

Schrével J (1971) Observations biologique et ultrastructurales sur les Selenidiidae et leurs conséquences sur la systématique des grégarinomophes. J Protozool **18**:448–470

Schrével J, Valigurová A, Prensier G, Chambouvet A, Florent I, Guillou L (2016) Ultrastructure of *Selenidium pendula*, the type species of archigregarines, and phylogenetic relations to other marine apicomplexa. Protist **167**:339–368

Seeber F, Steinfelder S (2016) Recent advances in understanding apicomplexan parasites. F1000Res 5:F1000 Faculty Rev-1369.

Smith TG, Walliker D, Ranford-Cartwright LC (2002) Sexual differentiation and sex determination in the Apicomplexa. Trends in Parasitol **18**:315–323

Talavera G, Castresana J (2007) Improvement of phylogenies after removing divergent and ambiguously aligned blocks from protein sequence alignments. Syst Biol **56**:564–577

Théodoridès J, Desportes I (1972) Mise en evidence de nouveaux représentants de la famille de Ganymedidae Huxley, grégarines parasites de crustacés. C R Acad Sci Paris **274(D)**:3251–3253.

Trifinopoulos J, Nguyen LT, von Haeseler A, Minh BQ (2016) W-IQ-TREE: a fast online phylogenetic tool for maximum likelihood analysis. Nucleic Acids Res **44**: W232–W235

Wakeman KC (2020) Molecular phylogeny of marine gregarines (Apicomplexa) from the Sea of Japan and the Northwest Pacific including the description of three novel species of *Selenidium* and *Trollidium akkeshiense* n. gen. n. sp. Protist 171:125710.

Wakeman KC, Leander BS (2012) Molecular phylogeny of Pacific Archigregarines (Apicomplexa), including descriptions of *Veloxidium leptosynaptae* n. gen., n. sp., from the sea cucumber *Leptosynapta clarki* (Echinodermata), and two new species of *Selenidium*. J Eukaryot Microbiol **59**:232–245

Wakeman KC, Leander BS (2013a) Identify of environmental DNA sequences using descriptions of four novel marine gregarine parasites, *Polyplicarium* n. gen. (Apicomplexa), from capitellid polychaetes. Mar Biodiv **43**:133–147

Wakeman KC, Leander BS (2013b) Molecular phylogeny of marine gregarine parasites (Apicomplexa) from tube-forming polychaetes (Sabellariidae, Cirratulidae, and Serpulidae), including descriptions of two new species of *Selenidium*. J Eukaryot Microbiol **60**:514–525

Wakeman KC, Reimer JD, Jenke-Kodama H, Leander BS (2014) Molecular phylogeny and ultrastructure of *Caliculium glossobalani* n. gen. et sp. (Apicomplexa) from a Pacific *Glossobalanus minutus* (Hemichordata) confounds the relationships between marine and terrestrial gregarines. J Eukaryot Microbiol **61**:343–353

Wallis JR, Smith AJR, Kawaguchi S (2017) Discovery of gregarine parasitism in some Southern Ocean krill (Euphausiacea) and the salp *Salpa thompsoni*. Polar Biol **40**:1913–1917